HHS Public Access

Author manuscript

Magn Reson Med. Author manuscript; available in PMC 2024 January 01.

Published in final edited form as:

Magn Reson Med. 2023 January ; 89(1): 276–285. doi:10.1002/mrm.29424.

Prospective Motion Correction in Kidney MRI Using Free Induction Decay Navigators

Cemre Ariyurek[1], **Tess E Wallace**[1], **Tobias Kober**[2,3,4], **Sila Kurugol**[1,*], **Onur Afacan**[1,*]

[1]Computational Radiology Laboratory, Department of Radiology, Boston Children's Hospital, Harvard Medical School, Boston, MA, United States

[2]Advanced Clinical Imaging Technology, Siemens Healthcare, Lausanne, Switzerland

[3]Department of Radiology, Lausanne University Hospital and University of Lausanne, Lausanne, Switzerland

[4]LTS5, École Polytechnique Fédérale de Lausanne (EPFL), Lausanne, Switzerland

Abstract

Purpose: Abdominal MRI scans may require breath-holding to prevent image quality degradation, which can be challenging for patients, especially children. In this study, we evaluate whether free induction decay navigators (FIDnavs) can be used to measure and correct for motion prospectively, in real-time.

Methods: FIDnavs were inserted into a 3D radial sequence with stack-of-stars sampling. MRI experiments were conducted on six healthy volunteers. A calibration scan was first acquired to create a linear motion model that estimates the kidney displacement due to respiration from the FIDnav signal. This model was then applied to predict and prospectively correct for motion in real-time during deep and continuous deep breathing scans. Resultant images acquired with the proposed technique were compared with those acquired without motion correction. Dice scores were calculated between inhale/exhale motion states. Furthermore, images acquired using the proposed technique were compared with images from XD-GRASP, a retrospective motion state binning technique.

Results: Images reconstructed for each motion state show that the kidneys' position could be accurately tracked and corrected with the proposed method. The mean of Dice scores computed between the motion states were improved from 0.93 to 0.96 using the proposed technique. Depiction of the kidneys was improved in the combined images of all motion states. Comparing results of the proposed technique and XD-GRASP, high quality images can be reconstructed from a fraction of spokes using the proposed method.

Conclusion: The proposed technique reduces blurriness and motion artifacts in kidney imaging by prospectively correcting their position both in-plane and through-slice.

Corresponding author: Cemre Ariyurek, Computational Radiology Laboratory, Boston Children's Hospital, 360 Longwood Avenue, Boston, MA 02215, cemre.ariyurek@childrens.harvard.edu, Tel: +1 6179191747.

*Sila Kurugol and Onur Afacan contributed equally to this work

Parts of this work were presented in the Joint Annual Meeting of ISMRM-ESMRMB in London, England, UK, 2022

Keywords

MRI motion correction; abdominal MRI; renal imaging; navigators; kidney MRI

1. Introduction

Abdominal MRI scans are widely used for the clinical assessment of several diseases[1,2,3]. These scans often require breath-holding to achieve sufficient image quality[4]. Free-breathing imaging with radial acquisition is relatively robust to motion compared to Cartesian acquisitions[5,6]. However, image quality is frequently degraded when imaging patients with irregular and deep breathing.

Although there are a number of prospective motion correction techniques for brain MRI[7,8], most motion correction (MoCo) techniques for abdominal MRI are based on retrospective correction such as respiratory phase binning[9,10], butterfly navigators[11], and discarding motion corrupted data[12]. However, techniques that correct for motion and use all of the acquired data are more efficient[13]. Moreover, all of these approaches use the center of radial k-space lines to detect motion, which is often inaccurate due to several factors including gradient delays[14], which result in inaccurate trajectories and errors in measuring k-space center. Furthermore, retrospective techniques require post-processing and images may not be immediately available.

Free induction decay navigators (FIDnavs) measure the k-space center directly without any spatial encoding and were used for motion detection for the first time by Brau et al. for prospective gating in abdominal MRI[15]. Later, multi-channel FIDnav signals were applied for head motion detection[16], retrospective head motion correction[17], real-time bulk motion detection-exclusion in abdominal MRI[14], and deliver accept/reject-and-reacquire decisions in carotid MRI[18].

Previous methods in abdominal MRI used FIDnavs only to track motion for gating, binning or motion detection but not for motion measurement and correction in real time. Also, previous techniques such as gating discards a large portion of acquired data, and increases acquisition time. Here, we propose a more efficient FIDnavs technique for prospective motion correction in abdominal MRI. The proposed method measures respiratory motion and corrects for it in real-time using FIDnavs. The FIDnav signal is first calibrated to the motion of the kidneys, which are assumed to move fairly rigidly during respiration[19], using a linear motion model and the acquisition is prospectively steered according to the predicted position of the kidneys. We tested our method on six healthy volunteers and assessed the quality of the images acquired with and without the proposed prospective motion correction.

The main contributions of this work are: (i) Prospectively correcting for motion in real-time by steering the imaging volume, (ii) Showing its applicability in kidney MRI, (iii) Using unencoded FIDnavs for motion measurement and correction which do not include any spatial encoding and are decoupled from the excited slab, enabling motion correction in the through-slice direction.

2. Methods

The proposed motion measurement and correction technique is summarized in Figure 1. Linear model parameters to translate FIDnav signals into estimates of kidney displacement were obtained from a prescan. The computed parameters were used for prospectively correcting kidney motion based on measured FIDnavs.

2.1. FID-navigated 3D radial stack-of-stars sequence

FIDnavs with separate non-selective RF pulses were inserted into a golden angle-ordered radial stack-of-stars sequence[20]. The pulse sequence diagram is shown in Supporting Information Figure S1A. In our stack-of-stars acquisition, all partitions are acquired sequentially for each rotation angle. FIDnav blocks with an ADC duration of 0.4 ms and a TE_{FIDnav} of 2 ms were acquired once for each rotation angle (i.e. every N_{par}), when $k_z=k_{zmax}$, increasing total acquisition time (TA) by $1/N_{par}$ percent. The flip angle of the non-selective FIDnav excitation pulse was matched to the flip angle of the imaging sequence. FIDnavs were used for both measuring and correcting motion in real-time.

2.2. Calibration

A prescan was used to calculate the linear model parameter that calibrates FIDnav to kidney displacement. Since the kidneys move rigidly along the psoas muscles[19], the dominant motion direction due to respiration is in the head-foot direction, followed by the anterior-posterior direction.

The prescan was acquired using a 3D radial stack-of-stars trajectory. The imaging volume was coronal-oblique and parallel to the longitudinal axis of the kidneys. Volunteers were asked to perform inhaling/exhaling alternatively every 5 seconds for a total of 50 seconds. In the scan, FIDnavs were acquired every ~50 ms.

For model calibration, the image corresponding to the central coronal-oblique slice of the calibration data was reconstructed using the non-uniform fast Fourier transform (NUFFT)[21] after applying a 1D Fourier transform in slice-selection direction. The coordinates of the uppermost point of the right kidney in the coronal-oblique plane were manually labeled on reconstructed slices with a temporal resolution of five seconds, corresponding to each exhale and inhale state denoted as S_i. The displacement of the kidney was denoted as Δd_{kidney} and was in the tilted z'-direction.

The correlation coefficients between kidney displacement and the magnitude of the FIDnavs measured by each coil ($FIDnav_{coilk}$) were computed and the spine coil element with the highest correlation coefficient was determined ($coil_{max}$):

$$coil_{max} = \left| corr(FIDnav_{coilk}(coil_k, S_i),\ \Delta d_{kidney}(S_i)) \right| \quad (1)$$

Here, *corr* denotes the correlation operation. Note that selecting a body matrix coil element is avoided since the body matrix coil is not fixed and can move with the subject's breathing. A linear motion model was used to estimate the translation in respiration direction:

$$\Delta d_{kidney}(t) = A \times (FIDnav_{coilmax}(t) - FIDnav_{coilmax}(t_0)) \quad (2)$$

where $FIDnav_{coilmax}(t_0)$ is the reference FIDnav measurement. The first N=50 spokes were ignored (i.e., t_0=N+1) to allow the FIDnav signal to reach steady-state. The value for the motion model parameter, A, was calculated and used as an input to the real-time motion correction exam along with the coil element identity with the highest correlation. Reconstructing calibration images, labeling the kidney position and computing parameters for the linear motion model took approximately two minutes.

2.3. Prospective motion correction

The coil identity number and calculated linear motion model parameter (A) were fed into the FID-navigated stack-of-stars sequence for prospective motion correction. To keep the same transmit and receive characteristics with the calibration, it was ensured that the shim settings were not adjusted between scans. The displacements estimated from the scaled FIDnav using the linear motion model were filtered using a 1D Kalman filter for robustness[7].

During the acquisition, MoCo was applied prospectively based on the 1D Kalman-filtered estimate of the kidney displacement using Eqn. 2.

In-plane motion was corrected by modifying the phase of the acquired k-space data. Through-slice motion was corrected by adjusting the frequency of the RF pulse.

2.4. MR Experiments

Six volunteers (3 female, 3 male, age=37.4±10.7 years) were scanned at 3T (MAGNETOM Prisma, Siemens Healthcare, Erlangen, Germany) following written, informed consent. Spine and body matrix coils were used with a total of 36 channels. For each volunteer, a calibration scan was acquired, prior to the real-time MoCo scan to determine the linear model parameters. Estimated model parameters were fed into scans with MoCo.

Calibration scan: Imaging parameters were as follows: TE/TR/FA = 1.49ms/4ms/9°, 16 coronal oblique slices with slice partial Fourier = 6/8, voxel size = 2.4x2.4x6mm^3, FOV = 300x300mm^2, receiver bandwidth = 930 Hz/px, 900 radial spokes, resulting in TA = 50 seconds.

Real-time motion correction experiments: Imaging parameters were TE/TR/FA = 1.49ms/4ms/9°, 32 coronal-oblique slices with slice partial Fourier = 6/8, voxel size = 1.2x1.2x3mm^3, FOV = 300x300mm^2, receiver bandwidth = 930 Hz/px and 1326 radial spokes, total scan time 2.5 minutes, designed to match our clinical abdomen protocol. In real-time MoCo scans, FIDnavs were acquired and MoCo parameters were updated every ~100 ms.

The following experiments were conducted:

1. *Deep breathing (DB) scan:* volunteers performed exhaling/inhaling with 10 seconds duration for each state.

2. *Continuous deep breathing (CDB) scan:* volunteers continuously exhaled/inhaled deeply.
3. *Shallow breathing (SB) scan:* volunteers tried to breathe shallowly and stay still.

DB and CDB scans were acquired with and without MoCo. A SB scan was acquired without MoCo as a reference. On one volunteer, the SB scan was repeated without FIDnavs embedded in the stack-of-stars sequence to investigate the effect of inserting FIDnavs on image quality.

Acquired scans were reconstructed using iGRASP[20], generating volumes for each inhale and exhale respiratory state, from 46 spokes (5 seconds) and 92 spokes (10 seconds) for CDB and DB, respectively.

Masks of right and left kidneys were generated from the center slices of the first exhale and inhale states. Dice scores between masks of kidneys segmented from inhale and exhale images were computed as a measure of overlap between kidneys. Higher Dice scores should indicate reduced misalignment due to motion and successful motion correction.

In addition, single volumes were reconstructed for each volunteer using a combination of all of the acquired spokes from multiple respiratory phases by NUFFT to evaluate the effectiveness of the proposed MoCo to reduce blurring.

NUFFT reconstructions of prospectively motion-corrected data (“MoCo On”) were compared to XD-GRASP[9] reconstructions of “MoCo Off” data. Four respiratory motion states were generated using XD-GRASP. The reconstructions were compared using the first 30%, 50%, 70% and 100% of spokes acquired in “MoCo On” and “MoCo Off” scans. Regularization parameter for XD-GRASP was selected based on the evaluation of an expert reader.

To investigate the robustness of the proposed MoCo technique, additional sets of experiments were performed as follows:

Experiment 1: Two volunteers were scanned by FID-navigated 3D stack-of-stars with axial orientation to demonstrate the proposed methods’ applicability to through-slice motion correction.

Experiment 2: The subject was asked to breathe irregularly during the scan to demonstrate the performance of the proposed method for irregular breathing patterns.

Experiment 3: The FIDnav calibration was trained while the volunteer performed shallow breathing but was asked to breathe deeply during the test scan to demonstrate the case where there is a mismatch in breathing patterns between the calibration and motion-corrected scan.

Experiment 4: The subject was asked to relax and move their arms and legs between calibration and test scan to demonstrate the performance of the proposed motion correction when the volunteer moves in between the calibration and motion-corrected scan.

Experiment 5: The k-space acquisition was changed from a 3D stack-of-stars trajectory to a cartesian trajectory to demonstrate applicability of this technique to Cartesian imaging.

3. Results

Oblique coronal images with and without FIDnavs are visually compared in Supporting Information Figure S1B. It can be observed that the scans yield similar image quality indicating that the insertion of FIDnavs into the sequence did not change the image quality.

Examples of fitted $FIDnav_{coilmax}$ and Kalman-filtered $FIDnav_{coilmax}$ (or equivalently applied MoCo) for deep breathing and continuous deep breathing are depicted in Figure 2A. Kalman filtering ensures accurate motion tracking while suppressing measurement noise.

GRASP reconstructions for inhale-exhale states and temporal evolution of reconstructed dynamic volumes for SB, DB, and CDB with and without MoCo are shown in Figure 2B for a representative volunteer. The temporal evolution of the reconstructed dynamic image series demonstrates that scans with MoCo have improved alignment of the kidneys over time.

Dice scores were improved for all volunteers, with the mean score increasing from 0.94 to 0.96 and 0.93 to 0.96 using MoCo for both DB and CDB experiments, respectively.

Single volume reconstructions combining all spokes for each volunteer are displayed in Figure 3. The proposed MoCo reduced blurriness and motion artifacts in kidneys by correcting their position during breathing in real-time.

Figure 4 and Supporting Information Figure S2 compare the XD-GRASP reconstructions when respiratory motion was binned into four states with the proposed motion correction method using 30%, 50%, 70% and 100% of spokes for coronal-oblique and axial imaging, respectively. In both coronal and axial imaging, depiction of the kidneys were improved with the proposed MoCo technique using only NUFFT reconstruction without any regularization for image reconstruction. However, the kidneys were still blurry in some motion states when XD-GRASP was applied despite using both motion binning and regularization during reconstruction. Moreover, image quality of XD-GRASP reconstructions was lower compared to the proposed prospective MoCo method since fewer spokes were used due to binning of motion states.

Irregular breathing patterns traced by the volunteer and corresponding reconstructed images with and without MoCo are shown in Figure 5A. XD-GRASP was applied to retrospectively correct for motion in the data acquired during irregular breathing (MoCo Off). Reconstructions of XD-GRASP and the proposed prospective MoCo technique are compared in Figure 5B. It can be observed that motion artifacts are reduced and image quality is improved using the proposed technique compared to XD-GRASP reconstruction in the case of irregular breathing.

The breathing patterns recorded by FIDnavs for the shallow breathing calibration and deep breathing scans with and without MoCo are shown in Supporting Information Figure S3A. Supporting Information Figure S3B demonstrates that motion artifacts are reduced with

application of real-time MoCo using model parameters obtained from the shallow breathing calibration scan.

Results of Experiments 4 and 5 are reported in Supporting Information Figures S4 and S5, respectively.

4. Discussion

To overcome image quality degradation and blurring in kidney MRI due to respiratory motion, we proposed to use FIDnavs to measure and prospectively correct for kidney displacement. Our results in volunteers demonstrate that respiratory motion can be accurately compensated in real-time using FIDnavs. Motion of the kidneys between inhale and exhale states can be clearly observed without MoCo and the alignment of the kidneys over time is substantially improved by the proposed MoCo. This visual assessment is supported quantitatively by a Dice score improvement between inhale/exhale frames.

Comparing the results of the proposed MoCo method and XD-GRASP, it can be observed that image quality is substantially improved using the proposed method, even though XD-GRASP benefits from regularization along the time while the proposed MoCo only uses NUFFT-based reconstruction without any regularization. This is partly because the proposed technique uses all of the acquired spokes to reconstruct one image, therefore is more time efficient. On the other hand, XD-GRASP bins the spokes into the number of motion states which essentially reduces the number of spokes used to reconstruct each motion state image by the same factor. In addition, there is some remaining uncorrected motion when spokes are binned to four motion states using XD-GRASP. To overcome this issue, the number of motion states could be increased; however, this would result in reduced image quality for each motion state due to using fewer spokes per state. Furthermore, another advantage of the proposed real-time MoCo technique is that the corrected images are available immediately at the end of the scan without delay and without requirement for iterative reconstruction as in XD-GRASP which takes longer (~5 min/slice). However, time spent in the calibration procedure required in the proposed method has to be taken into account (~2 min). Nevertheless, it is possible to continue the MRI exam with other scans that do not require motion correction.

Another advantage of the proposed prospective motion correction technique over retrospective correction is real-time steering in the through-slice direction by adjusting the frequency of the RF pulse to track the desired excitation volume. Without prospective motion correction, the outer slices may not be acquired consistently throughout the scan due to motion in the through-slice direction, which is not recoverable by retrospective techniques. In our axial imaging experiments, we successfully tracked the target volume in real-time by adjusting the RF pulse frequency to account for respiratory motion in the z-direction.

Inserting FIDnavs with their own RF pulse decouples FIDnav measurements from the excited slab, enabling motion correction in the through-slice direction, in exchange for a small increase in acquisition time compared to inserting FIDnavs within the imaging block.

Additionally, it does not alter the minimal TE or TR of the imaging block. Here, we demonstrate that acquiring FIDnavs every 100 ms is enough for accurate real-time motion correction and increases acquisition time by 4%. Moreover, we have shown that inserting FIDnavs does not affect image quality. There is approximately 10 ms latency of real-time information transfer between sequence and image calculation environment, which caused a latency of 3xTR (12 ms) in the real-time MoCo experiments.

In the calibration step, the need for manual labeling of a landmark point could limit the direct applicability of this technique in the clinic. Future work will concentrate on automated methods to measure kidney position in real-time, possibly using a fast deep learning method[22].

Consistency between the calibration and real-time MoCo scans is important since MoCo model parameters rely on the calibration scan. Hence, we investigated to what extent the proposed method is still effective when there is discrepancy in terms of motion displacement between the calibration and the prospective MoCo scans. The proposed technique was able to eliminate motion artifacts when the motion model parameters were obtained from a shallower breathing calibration scan and MoCo was applied on a deeper breathing scan.

It is possible for patients to breathe irregularly during the MRI scan which severely degrades image quality. Hence, a case for irregular breathing was tested in this work. It was observed that the proposed real-time MoCo technique reduces the motion artifacts and outperforms XD-GRASP in such a scenario.

Here, we applied the proposed MoCo technique to kidney imaging, but it can be adapted to other abdominal MRI scans by computing the linear motion model parameters for the target organ; however, the proposed method assumes that motion is fairly rigid with respiration, such as the liver. The remaining motion could be corrected retrospectively by nonrigid motion correction techniques[23,24].

5. Conclusion

In this study, we demonstrated that respiration-induced kidney motion can be measured and prospectively corrected by embedding FIDnavs into the sequence and training a linear motion model. We showed that respiratory motion could be accurately tracked using the linearized FIDnav motion model. Thus, the proposed motion correction technique could be beneficial to improve image quality in the presence of irregular or deep breathing with a potential reduction in scan time compared to respiratory gating.

Supplementary Material

Refer to Web version on PubMed Central for supplementary material.

Acknowlegments

This work was supported partially by the Society of Pediatric Radiology Multi-center Research Grant 2019 and by the NIDDK, NIBIB, NINDS and NLM of the National Institutes of Health under award numbers R01DK125561, R21DK123569, R21EB029627, R01NS121657, R01LM013608, R01EB019483, S10OD0250111 and by the grant

number 2019056 from the United States-Israel Binational Science Foundation (BSF), and a pilot grant from National Multiple Sclerosis Society under Award Number PP-1905-34002.

References

1. Notohamiprodjo M, Reiser MF, Sourbron SP. Diffusion and perfusion of the kidney. Eur J Radiol. 2010;76(3):337–347. [PubMed: 20580179]
2. Bartolozzi C, Lencioni R, Donati F, Cioni D. Abdominal MR: liver and pancreas. Eur Radiol. 1999;9(8):1496–1512. [PubMed: 10525857]
3. Horsthuis K, Lavini C, Stoker J. MRI in Crohn's disease. J Magn Reson Imaging. 2005;22(1):1–12. [PubMed: 15971179]
4. Chavhan GB, Babyn PS, Vasanawala SS. Abdominal MR imaging in children: motion compensation, sequence optimization, and protocol organization. Radiographics. 2013;33(3):703–719. [PubMed: 23674770]
5. Block KT, Chandarana H, Milla S, et al. Towards Routine Clinical Use of Radial Stack-of-Stars 3D Gradient-Echo Sequences for Reducing Motion Sensitivity. Journal of the Korean Society of Magnetic Resonance in Medicine. 2014;18(2):87. doi:10.13104/jksmrm.2014.18.2.87
6. Zhong X, Armstrong T, Gao C, et al. Accelerated k-space shift calibration for free-breathing stack-of-radial MRI quantification of liver fat and. Magn Reson Med. 2022;87(1):281–291. [PubMed: 34412158]
7. White N, Roddey C, Shankaranarayanan A, et al. PROMO: Real-time prospective motion correction in MRI using image-based tracking. Magn Reson Med. 2010;63(1):91–105. [PubMed: 20027635]
8. Maclaren J, Herbst M, Speck O, Zaitsev M. Prospective motion correction in brain imaging: a review. Magn Reson Med. 2013;69(3):621–636. [PubMed: 22570274]
9. Feng L, Axel L, Chandarana H, Block KT, Sodickson DK, Otazo R. XD-GRASP: Golden-angle radial MRI with reconstruction of extra motion-state dimensions using compressed sensing. Magn Reson Med. 2016;75(2):775–788. [PubMed: 25809847]
10. Cruz G, Atkinson D, Buerger C, Schaeffter T, Prieto C. Accelerated motion corrected three-dimensional abdominal MRI using total variation regularized SENSE reconstruction. Magn Reson Med. 2016;75(4):1484–1498. [PubMed: 25996443]
11. Cheng JY, Alley MT, Cunningham CH, Vasanawala SS, Pauly JM, Lustig M. Nonrigid motion correction in 3D using autofocusing with localized linear translations. Magn Reson Med. 2012;68(6):1785–1797. [PubMed: 22307933]
12. Coll-Font J, Afacan O, Chow JS, et al. Bulk motion-compensated DCE-MRI for functional imaging of kidneys in newborns. Journal of Magnetic Resonance Imaging. 2020;52(1):207–216. doi:10.1002/jmri.27021 [PubMed: 31837071]
13. Odille F, Uribe S, Batchelor PG, Prieto C, Schaeffter T, Atkinson D. Model-based reconstruction for cardiac cine MRI without ECG or breath holding. Magnetic Resonance in Medicine. 2010;63(5):1247–1257. doi:10.1002/mrm.22312 [PubMed: 20432296]
14. Stemkens B, Benkert T, Chandarana H, et al. Adaptive bulk motion exclusion for improved robustness of abdominal magnetic resonance imaging. NMR Biomed. 2017;30(11). doi:10.1002/nbm.3830
15. Brau ACS, Brittain JH. Generalized self-navigated motion detection technique: Preliminary investigation in abdominal imaging. Magn Reson Med. 2006;55(2):263–270. [PubMed: 16408272]
16. Kober T, Marques JP, Gruetter R, Krueger G. Head motion detection using FID navigators. Magn Reson Med. 2011;66(1):135–143. [PubMed: 21337424]
17. Wallace TE, Afacan O, Waszak M, Kober T, Warfield SK. Head motion measurement and correction using FID navigators. Magnetic Resonance in Medicine. 2019;81(1):258–274. doi:10.1002/mrm.27381 [PubMed: 30058216]
18. Dyverfeldt P, Deshpande VS, Kober T, Krueger G, Saloner D. Reduction of motion artifacts in carotid MRI using free-induction decay navigators. J Magn Reson Imaging. 2014;40(1):214–220. [PubMed: 24677562]

19. Moerland MA, van den Bergh AC, Bhagwandien R, et al. The influence of respiration induced motion of the kidneys on the accuracy of radiotherapy treatment planning, a magnetic resonance imaging study. Radiother Oncol. 1994;30(2):150–154. [PubMed: 8184113]

20. Feng L, Grimm R, Block KT, et al. Golden-angle radial sparse parallel MRI: combination of compressed sensing, parallel imaging, and golden-angle radial sampling for fast and flexible dynamic volumetric MRI. Magn Reson Med. 2014;72(3):707–717. [PubMed: 24142845]

21. Fessler JA, Sutton BP. Nonuniform fast fourier transforms using min-max interpolation. IEEE Transactions on Signal Processing. 2003;51(2):560–574. doi:10.1109/tsp.2002.807005

22. Haghighi M, Warfield SK, Kurugol S. AUTOMATIC RENAL SEGMENTATION IN DCE-MRI USING CONVOLUTIONAL NEURAL NETWORKS. Proc IEEE Int Symp Biomed Imaging. 2018;2018:1534–1537. [PubMed: 30473744]

23. Odille F, Vuissoz PA, Marie PY, Felblinger J. Generalized reconstruction by inversion of coupled systems (GRICS) applied to free-breathing MRI. Magn Reson Med. 2008;60(1):146–157. [PubMed: 18581355]

24. Usman M, Atkinson D, Odille F, et al. Motion corrected compressed sensing for free-breathing dynamic cardiac MRI. Magn Reson Med. 2013;70(2):504–516. [PubMed: 22899104]

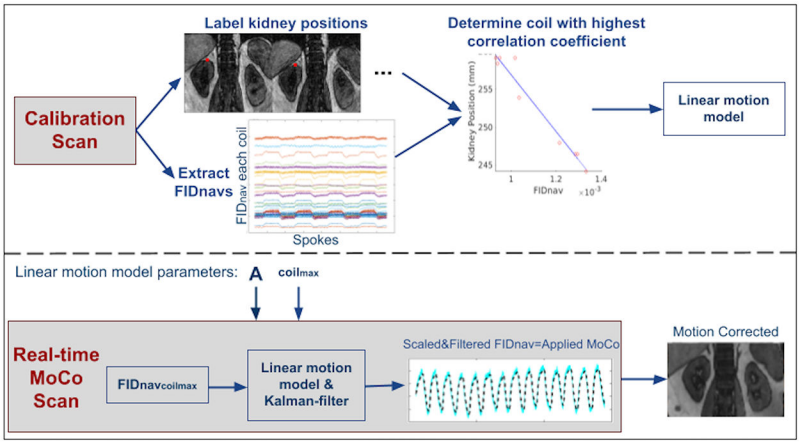

Figure 1.

Overview of the proposed prospective motion correction technique. Calibration Scan: Volunteers performed inhaling/exhaling every 5 seconds alternatively for a total of 50 seconds. The calibration data was reconstructed and processed immediately following the prescan. Kidney positions were labeled from NUFFT reconstructed images for each inhale/exhale frame. The linear motion model parameter A in Eqn. 2 was determined from the FIDnavs measured by the coil yielding the highest correlation with the kidney displacement over time. Real-time MoCo Scan: The determined linear translation parameter and coil identity number ($coil_{max}$) were used in the real-time MoCo scans. FIDnavs of $coil_{max}$ was scaled and 1D Kalman-filtered in the vendor image calculation environment, and motion estimates were passed to the correction module in the sequence, which updated the applied gradients and RF pulses to compensate for translational motion.

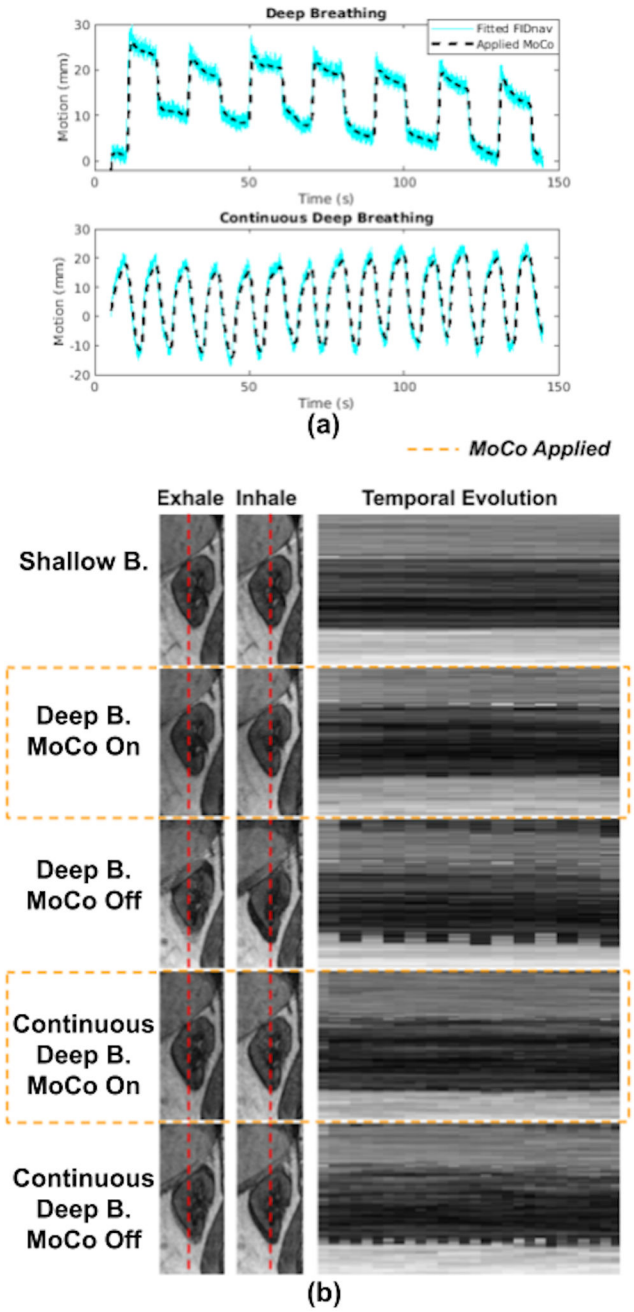

Figure 2.

(a) Fitted FIDnavs, equivalent to estimated kidney displacement using Eqn. 2, and applied MoCo, equivalent to 1D Kalman-filtered fitted FIDnavs, for deep breathing and continuous deep breathing with MoCo scans for one volunteer. The gain of the Kalman-filter was empirically set to 0.033 considering a trade-off between noise suppression for robustness and accurate motion tracking. (b) Temporal evolution of a line of voxels from one kidney over shallow, deep and continuous deep breathing with and without MoCo scans for one volunteer. The leftmost column shows the images of the kidney with a red line indicating the

selected line of voxels plotted time evolution on the right. Images acquired with MoCo show better aligned series of volumes over time.

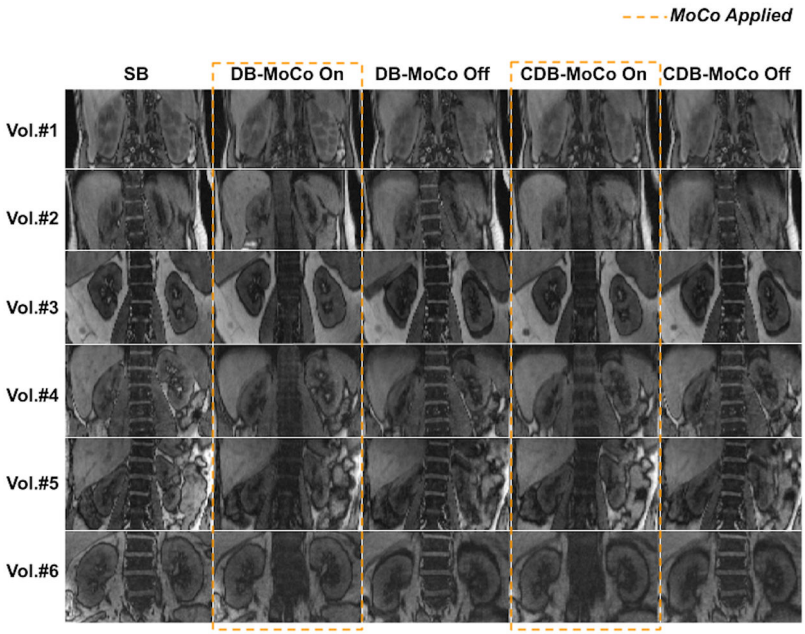

Figure 3.

NUFFT reconstructions obtained from all 1326 radial spokes for all volunteers for shallow breathing (SB), deep breathing (DB) and continuous deep breathing (CDB) with and without MoCo scans. Motion artifacts and blurring in kidneys are reduced using MoCo.

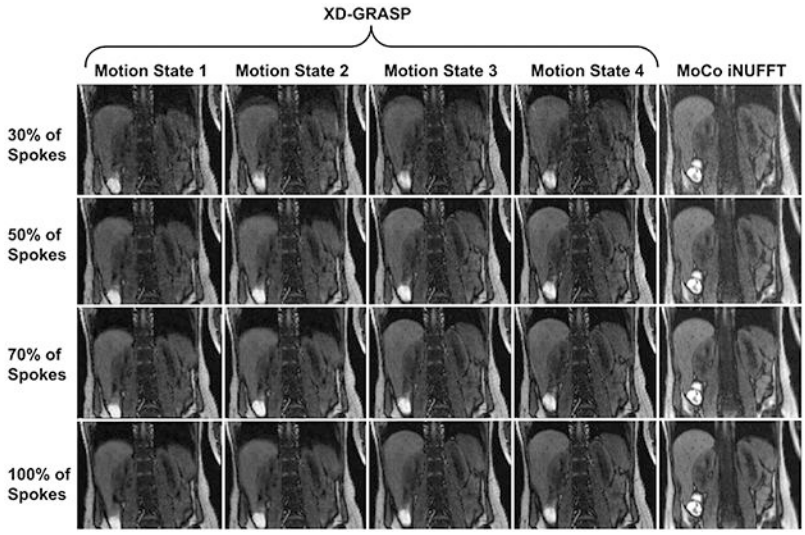

Figure 4.

Comparison with XD-GRASP with regularization applied along temporal direction. The proposed method (MoCo NUFFT) uses all of 30%, 50%, 70%, 100% of spokes acquired in each row, respectively, and reconstructs a single motion-corrected image without employing any regularization. Whereas, XD-GRASP bins the spokes into number motion states which essentially reduces the number used to reconstruct each motion state image by the same factor. Here, motion was resolved into four respiratory states. Although increasing the number of motion states could decrease the motion artifacts, it would decrease the image quality as well. Hence, the proposed technique is more efficient compared to XD-GRASP since it uses all of 30%, 50%, 70%, 100% of the spokes in each row. Therefore, 30% of the scan is sufficient for the required image quality using the proposed MoCo.

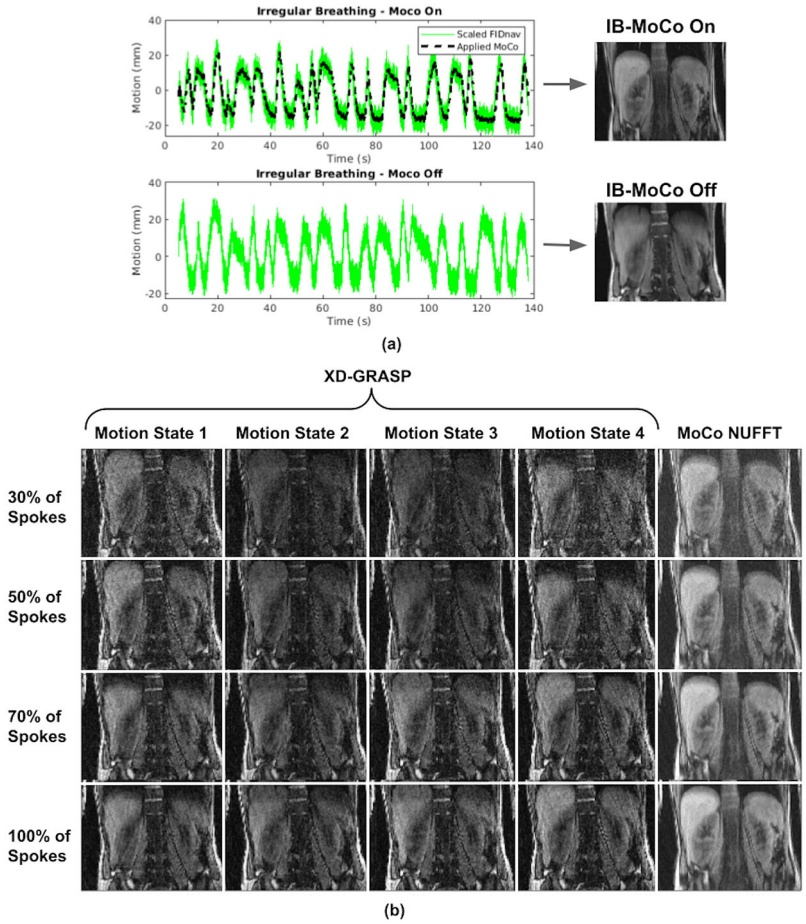

Figure 5.

Results of the irregular breathing experiment. (a) Breathing patterns measured by FIDnav are shown for MoCo On and MoCo Off scans, and applied motion correction for the MoCo scan. (b) NUFFT reconstructions obtained from all 1326 radial spokes for shallow breathing (SB) and irregular breathing (IB) with and without MoCo scans. Despite very irregular and deep breathing patterns, the proposed prospective MoCo technique reduced the motion artifacts. **(b)** Comparison of proposed method (MoCo NUFFT) with XD-GRASP with regularization along temporal direction for irregular breathing experiment. XD-GRASP method results in noisier images because it uses fewer spokes due to sorting of the spokes into respiratory phases compared to the proposed prospective MoCo technique which effectively uses all spokes. Even when using 30% of all spokes (top row), the proposed technique can generate improved quality images compared to XD-GRASP. Note that the parameters for XD-GRASP had to be hand-tuned and optimized to be able to correctly capture the breathing pattern for the specific volunteer for obtaining the reported results.